



Switched Systems and Applications to Mutual Synchronization

Andrea Espinel[‡] and Ina Taralova[†]

[†]IRCCyN UMR CNRS 6597, Ecole Centrale de Nantes

1 Rue de la Noë, 44321 Nantes Cedex, France

Email: andrea.espinel@irccyn.ec-nantes.fr, ina.taralova@irccyn.ec-nantes.fr

Abstract– This paper deals with the challenging problem of mutual synchronization of discrete-time chaotic systems. This particular type of synchronization allows to model successfully the complex dynamics of diverse systems, such as ecological, economical, physical, chemical etc. Unlike the usual master-slave synchronization, here we consider bidirectionally connected sub-systems with identical priority. Switched Luenberger observers are designed to carry out the mutual synchronization, and their performances are compared in the cases with, and without gaussian noise.

1. Introduction

Mutual synchronization describes a large variety of phenomena ranging from physics and biology to engineering and social sciences. Unidirectional and bidirectional synchronization of continuous time chaotic systems has been investigated in [1,2], fewer papers have been devoted to discrete time systems [3,4].

In [9], the problem of the classical unidirectional master-slave synchronization has been reformulated from control theory point of view, in terms of (non) linear observer design. The novelty in the present paper is that unlike the above master-slave configuration, here the synchronization is to be achieved bidirectionally, using two symmetrical observers (one for each subsystem). The idea is to exploit the richness of the nonlinear dynamics: for identical parameters, the system can exhibit qualitatively different behaviors (multistability), such as periodic, chaotic etc according to the initial conditions. This provides the challenging opportunity to analyze the mutual synchronization between two subsystems, which have been tuned to different orbits, but also between subsystems with slightly different parameters. The latter assumption can be used to model physical systems subject to ageing, temperature variations etc.

The function that has been chosen as an application example in this paper has already shown its excellent properties as an Efficient Chaotic Pseudo Random Number Generators (CPRNG). It uses chaotic sampling and ultra weak coupling which beats most of the classical random number generators [5].

2. System Definition

The system under consideration has been introduced for the first time by Lozy in [6]. It can be written as

$$x(n+1) = f(x(n)) = A \Lambda(x(n)) \quad (1)$$

For a second order system, the matrix A is defined by:

$$A = \begin{pmatrix} (1 - \epsilon_1) & \epsilon_1 \\ \epsilon_2 & (1 - \epsilon_2) \end{pmatrix}$$

and Λ is the tent function evaluated by the components of the vector $x \in [-1,1]^2$:

$$\Lambda(x) = sx + 1, \quad s = \begin{cases} 2, & x < 0 \\ -2, & \text{else} \end{cases} \quad (2)$$

However, state-space representation of the system is more convenient for control theory analysis [5]. Taking into consideration that the system is also a switched piecewise affine system, it can be expressed as

$$\begin{aligned} x(n+1) &= A_n x(n) + B \\ y(n) &= Cx(n) \end{aligned} \quad (3)$$

where s_{10} is associated to x_1 and s_{20} to x_2 (see eq.2):

$$A_n = \begin{pmatrix} (1 - \epsilon_1)s_{10} & \epsilon_1 s_{20} \\ \epsilon_2 s_{10} & (1 - \epsilon_2)s_{20} \end{pmatrix}, B = \begin{pmatrix} 1 \\ 1 \end{pmatrix}$$

It comes that the phase plane is divided into four different regions with locally linear behavior.

2.1. Analysis of the System

The chaoticity of the system depends on the choice of ϵ_1 and ϵ_2 . The fixed points determination has been completed by the parameter plane analysis to establish the chaotic regions in the parameter plane. Fixed points are defined by:

$$\begin{aligned} x_1(n) &= (1 - \epsilon_1)s_{10}x_1(n) + \epsilon_1 s_{20}x_2(n) + 1 \\ x_2(n) &= \epsilon_2 s_{20}x_2(n) + (1 - \epsilon_2)s_{20}x_2(n) + 1 \end{aligned} \quad (4)$$

Then, each component can be defined in function of the system parameters.

As the values of s depend on the two components (x_1, x_2) , the fixed points determination have been studied independently in the four regions of the phase plane. The analysis gives two fixed points. In the region $x_1 \in [-1; 0]$, $x_2 \in [-1; 0]$, the coordinates of the

fixed point are $(-1,-1)$. In the region $x_1 \in [0; 1]$, $x_2 \in [0; 1]$, the fixed point is located at $(1/3, 1/3)$.

Hereafter we are interested in the second fixed point whose Jacobean eigenvalues are $((-2, 2(-1 + \epsilon_1 + \epsilon_2)))$. It is a saddle between $0.5 \leq \epsilon_1 + \epsilon_2 \leq 1.5$ and an unstable node outside.

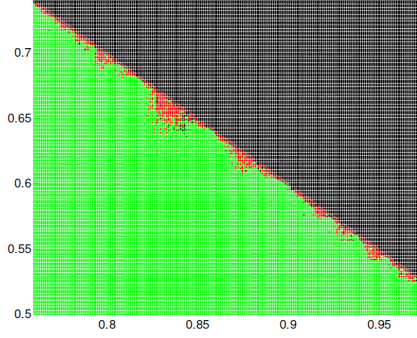


Figure 1. Parameter plane (ϵ_1, ϵ_2) of the Lozi system. (1)

Figure 1 shows the parameter plane (ϵ_1, ϵ_2) of the system. The parameter plane sweeping is highly sensitive to the numerical precision, and therefore is not easy to interpret. Thus, the green color is supposed to indicate a convergence towards the fixed point $(-1,-1)$ that is unstable, but numerically attractive; this problem can be avoided using a weak parameter coupling [8]. The black color indicates the chaotic behavior, and the red line corresponds to the fixed point $(1/3, 1/3)$, which bifurcates at $\epsilon_1 + \epsilon_2 = 1.5$.

The inverse map of the system is given by:

$$x(n) = f^{-1}(x(n+1)) = A_n^{-1}(x(n+1) + B) \quad (5)$$

with:

$$A_n^{-1} = \begin{pmatrix} \frac{\epsilon_2 - 1}{(\epsilon_1 + \epsilon_2 - 1)s_{10}} & \frac{1}{s_{10}} - \frac{\epsilon_2 - 1}{(\epsilon_1 + \epsilon_2 - 1)s_{10}} \\ \frac{\epsilon_2}{(\epsilon_1 + \epsilon_2 - 1)s_{20}} & \frac{\epsilon_1 - 1}{(\epsilon_1 + \epsilon_2 - 1)s_{20}} \end{pmatrix}$$

Furthermore, the line $x_1(n) = x_2(n)$ is associated with the stable manifold of the saddle fixed point $(1/3, 1/3)$. The diagonal is invariant for the recurrence, and its preimage is the anti-diagonal $x_1(n) = -x_2(n)$. For both of them we obtained the one dimensional Lozi map:

$$x_1(n+1) = x_2(n+1) = s_{10}x_1(n) + 1 \quad (6)$$

3. Mutual Synchronization

Unlike [7], here we do not deal with the classical master slave synchronization of the Lozi system, but we are interested in the bidirectional coupling of two connected Lozi subsystems, and their synchronization towards different type of orbits (fixed point or chaotic

behavior). To do this, a Luenberger observer has been used for the estimation of x .

$$\hat{x}(n+1) = \hat{A}\hat{x}(n) + B + K(\hat{y}(n) - y(n)) \quad (7)$$

Now, to achieve the mutual synchronization, an observer has been designed for each subsystem, called $x^M(n+1)$ and $x^S(n+1)$. It should be noted that the super script M and S are chosen for convenience, but they do not indicate here any hierarchy. Thus, the two subsystems are now modeled by:

$$\begin{aligned} x^M(n+1) &= A x^M(n) + K(y^M(n) - y^S(n)) \\ x^S(n+1) &= A x^S(n) + K(y^S(n) - y^M(n)) \end{aligned} \quad (8)$$

The gain K is the same for both subsystems and determines the dynamics of the error defined by:

$$e(n) = x^M(n) - x^S(n) \quad (9)$$

that is equivalent in the opposite direction $x^M(n) - x^S(n)$. Then, the matrix that governs the error dynamics is calculated as follows:

$$\begin{aligned} e(n+1) &= A(x^M(n) - x^S(n)) + 2K(y^M(n) - y^S(n)) \\ e(n+1) &= (A + 2KC)e(n) \end{aligned} \quad (10)$$

The asymptotic convergence of the synchronization error is guaranteed if the error matrix has eigenvalues in the unit circle. The exact (finite time) convergence is achieved when the eigenvalues are at the origin. The aim is to find the values of K that synchronize both subsystems. As the error matrix is of second order, it can be achieved in two steps. Therefore, it has to be independent of the way of switching between the four regions of the plane. For $i \in \{1; 4\}, j \in \{1; 4\}$:

$$(A_i + 2K_i C)(A_j + 2K_j C) = 0 \quad (11)$$

The solution for the matrix K presented in [7], has been adapted to the mutual synchronization:

For $x_1 \in [0; 1], x_2 \in [0; 1]$:

$$A_1 = 2 * \begin{pmatrix} -(1 - \epsilon_1) & -\epsilon_1 \\ -\epsilon_2 & -(1 - \epsilon_2) \end{pmatrix} \quad K_1 = \begin{pmatrix} 2 - \epsilon_1 - \epsilon_2 \\ \frac{1 - 2\epsilon_2 + \epsilon_2^2 + \epsilon_1\epsilon_2}{\epsilon_1} \end{pmatrix}$$

for $x_1 \in [-1; 0], x_2 \in [0; 1]$:

$$A_2 = 2 * \begin{pmatrix} 1 - \epsilon_1 & -\epsilon_1 \\ \epsilon_2 & -(1 - \epsilon_2) \end{pmatrix} \quad K_2 = \begin{pmatrix} \epsilon_1 - \epsilon_2 \\ \frac{1 - 2\epsilon_2 + \epsilon_2^2 - \epsilon_1\epsilon_2}{\epsilon_1} \end{pmatrix}$$

for $x_1 \in [-1; 0], x_2 \in [-1; 0]$:

$$A_3 = -A_1 \quad K_3 = -K_1$$

and for $x_1 \in [0; 1], x_2 \in [-1; 0]$:

$$A_4 = -A_2 \quad K_4 = -K_2 \quad (12)$$

4. Results and Discussion

The first analysis deals with the synchronization of two identical chaotic subsystems (same parameters), starting from different initial conditions (belonging to different locally linear regions). The evolution of the error between $x_2^M - x_2^S$, shown in Figure 2, illustrates the exact convergence for $(\epsilon_1, \epsilon_2) = (0.3, 0.1)$ for both subsystems, and initial conditions $(x_1^M(0), x_2^M(0)) = (0.154, 0.289)$; $(x_1^S(0), x_2^S(0)) = (0.131, -0.085)$.

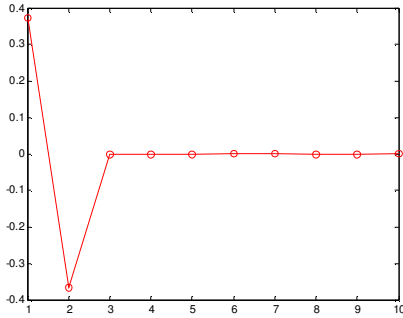


Figure 2: Evolution of the difference between x_2^M and x_2^S for the first ten iterations: exact synchronization.

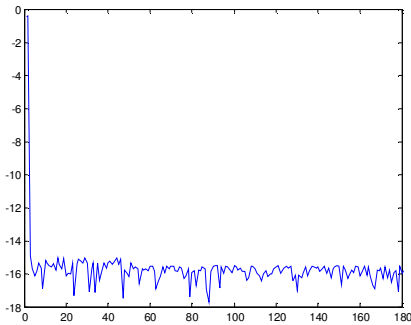


Figure 3. Quadratic synchronization error, exact observer.

Figure 3 shows the exact quadratic synchronization error, and Figure 4 the quadratic synchronization error using an asymptotic observer with both poles placed at 0.9. It can be seen for Fig.2 that even though the two subsystems start from two different regions, the exact convergence is obtained in only two iterations as in the case of the classical master-slave synchronization [7]. The synchronization error

$$e = \sqrt{(x_1^M - x_1^S)^2 + (x_2^M - x_2^S)^2} \quad (13)$$

is quite satisfactory (10^{-15} , which is close to the computer precision). In the case of asymptotic observer the synchronization is reached as well, but the convergence is much slower (Fig.4). Moreover, the performed tests have shown that unlike the expectations, the asymptotic observer did not outstand the exact observer in the presence of noise.

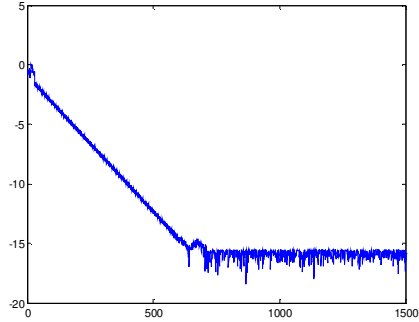


Figure 4. Quadratic synchronization error, asymptotic observer.

The Lozi system is very complex and exhibits most of the features characterizing nonlinear dynamical systems, such as the extreme sensitivity to the initial conditions and small parameters variations, and multistability: coexistence of fixed point and chaotic attractor has been found at the bifurcation line $\epsilon_1 + \epsilon_2 = 1.5$. Since the map has no stable fixed point, the saddle fixed point $(1/3, 1/3)$ has been selected to test the bidirectional synchronization. The saddle fixed point has been reached, initializing the first subsystem at the stable manifold, taking the initial conditions from f^{-1} . In this particular case, it easily achievable, because the first low rank preimages of the fixed point $(1/3, 1/3)$ lie on the diagonal $x_1(n) = x_2(n)$, which is invariant by the map f , and also the preimage of the diagonal is the anti-diagonal $x_1(n) = -x_2(n)$, as already shown.

It should be noted that parameters have been tuned outside the usual parameter range of weak coupling [8], but this choice has been done deliberately, in order to analyze the mutual synchronization for different coexisting dynamical behaviors.

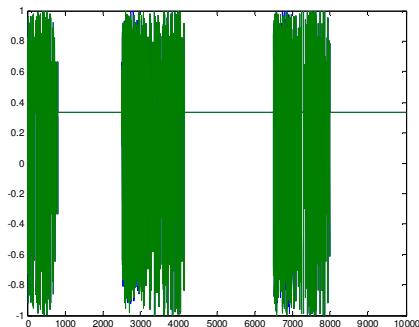


Figure 5. Exact synchronization between two subsystems (fixed point - chaotic attractor; identical parameters: alternated white noise).

Figure 5 and Figure 6 show the exact synchronization and the quadratic error between two subsystems with identical parameters. The first one was tuned to exhibit a fixed point trajectory and the second one a chaotic trajectory. The initial conditions for the fixed point had

been chosen on the stable manifold, using the low rank preimages. After the synchronization, both subsystems converge towards the fixed point $(1/3, 1/3)$ which turns out to be attractive after the synchronization. The same parameters have been chosen for both subsystems $(\epsilon_1, \epsilon_2) = (0.88, 0.62)$, i.e. at the bifurcation line $\epsilon_1 + \epsilon_2 = 1.5$ and synchronization has been obtained for different “master” and “slave” initial conditions $(x_1^M(0), x_2^M(0)) = (0.17, 0.25); (x_1^S(0), x_2^S(0)) = (0.222, 0.429)$. Therefore, besides achieving the successful synchronization, it could be argued that the observer might have a stabilizing effect on the overall system’s behavior.

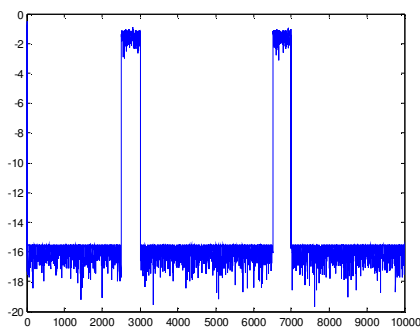


Figure 6. Quadratic synchronization error. (13)

In addition, Gaussian white noise has been added between (2500,3000) and (6500,7000) with 5% amplitude in order to test the robustness of the observers in presence of noise. The obtained results show that the system resynchronizes back successfully when the noise has been removed. Compared to Fig. 6, the perturbation time intervals are longer in Fig. 5 because after the noise removal, there is a chaotic transient before the subsystems resynchronize at the fixed point. On the other hand, the noise could not be rejected; unlike the expectations, qualitatively similar results had been obtained with the asymptotic observer (not shown here for lack of space).

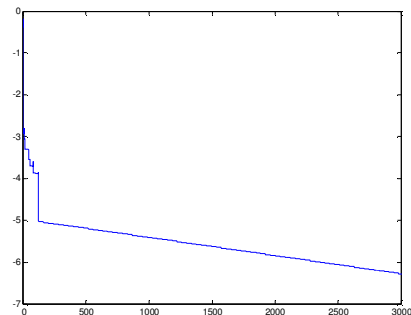


Figure 7. Synchronization error between the two subsystems tuned at fixed point and chaotic attractor (slightly different parameters).

Figure 7 shows the synchronization results for the same “master” but another choice of initial conditions and

parameters for the “slave”. It exhibits again a chaotic behavior for $(x_1^S(0), x_2^S(0)) = (-0.189, 0.437)$ and in addition, a small variation of $\epsilon_2 \Delta\epsilon_2 = (10^{-2})$ has been applied: $(\epsilon_1, \epsilon_2) = (0.88, 0.619)$. The synchronization is successfully achieved again, but towards the chaotic behavior; the chaotic attractor lies on the diagonal $x_1 = x_2$. The quadratic synchronization error is represented in Fig. 7. If noise is added, the results are qualitatively similar to those in Fig. 6.

Conclusion

Mutual synchronization of two Lozi subsystems has been designed using symmetric Luenberger observers. Two different kind of observers have been used, exact and asymptotic one, and their performances have been tested in presence of noise. It has been shown that the two subsystems synchronize successfully when they start from different initial conditions, exhibit different permanent regimes, or have different parameters. Current works are carried out to generalize the results for more than two connected subsystems.

Acknowledgements

The authors would like to thank prof. Fournier-Prunaret et prof. Lozi for their useful suggestions and comments during the preparation of this paper.

References

- [1] ZM Ge, YS Chen, “Adaptive synchronization of unidirectional and mutual coupled chaotic systems”, *Chaos, Solitons and Fractals*, vol. 26, pp. 881–888, 2005.
- [2] Y Yu, S Zhang, “The synchronization of linearly bidirectional coupled chaotic systems”, *Chaos, Solitons and Fractals*, vol.22, pp.189–197, 2004.
- [3] M. Cencini, A. Torcini, “Nonlinearly driven transverse synchronization in coupled chaotic systems”, *Physica D*, vol.208, pp.191-208,2005.
- [4] I. Matskiv, Y. Maistrenko, E. Mosekilde, “Synchronization between interacting ensembles of globally coupled chaotic maps”, *Physica D*, vol.199, pp.45-60,2004.
- [5] S. Hénaff, I. Taralova et R. Lozi, “Statistical and spectral analysis of a new weakly coupled maps system”, *Indian Journal of Industrial and Applied Mathematics*, vol 2.N°2, pp. 1-17, 2009.
- [6] R. Lozi, “New enhanced chaotic number generators”, *Indian Journal of Industrial and Applied Mathematics*, vol.1, pp. 1-23, 2008.
- [7] S. Hénaff, I. Taralova et R. Lozi, “Exact and asymptotic synchronization of a new weakly coupled map”, *Journal of Nonlinear Systems and Applications*, vol 1 (2), 2010.
- [8] R. Lozi, “Emergence of Randomness from Chaos”, to appear in: *International Journal of Bifurcations and Chaos*.
- [9] H. Nijmeijer, “A dynamical control view on synchronization”, *Physica D*, vol.154, pp. 219–228, 2001.